Pareto-Optimality-Based Constraint-Handling Technique and Its Application to Compressor Design

Akira Oyama[*] Kozo Fujii[†]
Institute of Space and Astronautical Science / JAXA, Sagamihara, Kanagawa, 229-8510, Japan

Koji Shimoyama[‡]
University of Tokyo, Bunkyo, Tokyo, 113-8656, Japan

and

Meng-Sing Liou[§]
NASA Glenn Research Center, Cleveland, Ohio, 44135

A new constraint-handling technique based on Pareto-optimality concept is proposed for evolutionary algorithms to efficiently deal with multiobjective multi-constraint design optimization problems. The essence of the proposed method is to apply non-dominance concept based on constraint function values to infeasible designs and to apply non-dominance concept based on objective function values to feasible designs. The proposed technique does not need any constants to be tuned as the proposed technique does not use weighted-sum of constraints. First, the proposed approach is demonstrated to be remarkably more robust than traditional constraint-handling techniques through the optimal design of a welded beam and conceptual design optimization of a two-stage-to-orbit space plane. Next, high-fidelity aerodynamic design optimization of an axial compressor blade design is demonstrated.

Nomenclature

l_{max}	=	number of design variables
m_{max}	=	number of objective functions
n_{max}	=	number of constraint functions
$\vec{x} = (x_1,...,x_l,...,x_{l_{\max}})$	=	design variable vector of a design,
$f_1(\vec{x}),...,f_m(\vec{x}),...f_{m_{\max}}(\vec{x})$	=	objective functions
$g_1(\vec{x}) < 0,...,g_n(\vec{x}) < 0,...g_{n_{\max}}(\vec{x}) < 0$	=	constraints
a_m	=	objective function weight coefficients, $m=1,...,m_{max}$
b_n	=	penalty function weight coefficients, $n=1,...,n_{max}$

[*] Research Associate, Department of Space Transportation Engineering, 3-1-1 Yoshinodai, Member AIAA.
[†] Professor, Department of Space Transportation Engineering, 3-1-1 Yoshinodai, Fellow AIAA.
[‡] Ph.D. student, Department of Aeronautics and Astronautics, Fujii Lab., 3-1-1 Yoshinodai, Sagamihara, Kanagawa, 229-8510, Japan, Student Member AIAA.
[§] Senior Scientist, Turbomachinery and Propulsion Systems Division, 21000 Brookpark Road MS 5-11, Associate Fellow AIAA.

I. Introduction

MOST of multidisciplinary design optimization problems are multiobjective and multi-constraint design optimization problems. For example, a typical transonic aircraft wing design involves minimization of mission block fuel, maximum take-off weight, Mach divergence drag, and wing box weight while constraints on flutter speed, structural strength, manufacturing capability, fuel tank volume, etc. must be met. Another example is the supersonic transportation design[1], which has four objectives (drag coefficients at transonic and supersonic cruise speeds, wing root bending moment and pitching moment) and constraints on lift coefficients at transonic and supersonic cruise speeds as well as wing thickness. Many other multiobjective and multi-constraint design optimization problems are easily found, such as low-boom supersonic business jet[2], expendable launcher[3], and multistage compressor[4].

A multiobjective optimization problem (MOP) simultaneously involves several competing objectives. While a single objective optimization problem may have a unique optimal solution, MOPs present a set of compromised solutions, largely known as the tradeoff surface, *Pareto-optimal* solutions or *non-dominated* solutions[1]. These solutions are optimal in the sense that no other solutions in the search space are superior to them when all objectives are considered (Fig. 1). The goal of MOPs is to find as many Pareto-optimal solutions as possible to reveal tradeoff information among different objectives. Once such solutions are obtained, the higher-level decision-maker will be able to choose a final design with further considerations.

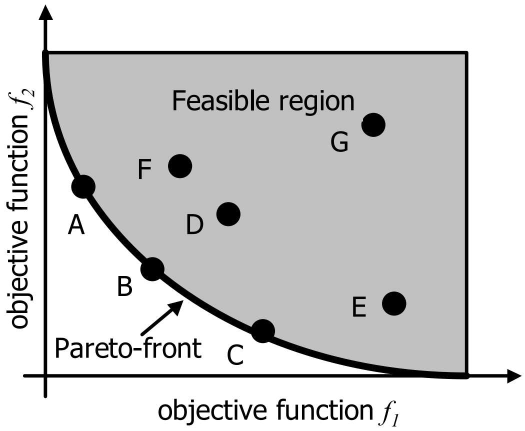

Figure 1. The concept of Pareto-optimality. *This is an example of MOPs, which minimizes two conflicting objectives f_1 and f_2. This MOP has innumerable compromised Pareto-optimal solutions such as solutions A, B, and C. These solutions are optimal in the sense that there is no better solution in both objectives. One cannot say which is better among these Pareto-optimal solutions because improvement in one objective degrades another.*

Traditional design methods such as the gradient-based methods[5] are single objective optimization methods that optimize only one objective. These methods usually start with a single baseline design and use local gradient information of the objective function with respect to changes in the design variables to calculate a search direction. When these methods are applied to a MOP, the problem is transformed into a single objective optimization problem by combining multiple objectives into a single objective typically using a weighted sum method. For example, to minimize objective functions f_1 and f_2, these objective functions are combined into a scalar function F as;

$$F(\vec{x}) = a_1 \cdot f_1(\vec{x}) + a_2 \cdot f_2(\vec{x}),\ a_1 + a_2 = 1 \quad (1)$$

Then fitness of each design is determined based on the F value. This approach, however, can find only one of the Pareto-optimal solutions corresponding to each set of the weights a_1 and a_2. Therefore, one must run many optimizations by trial and error adjusting the weights to get Pareto-optimal solutions uniformly over the potential Pareto-front. This is considerably time consuming in terms of human time. What is more, there is no guarantee that uniform Pareto-optimal solutions can be obtained. For example, when this approach is applied to a MOP that has concave tradeoff surface, it converges to two extreme optimums without showing any tradeoff information between the objectives (Fig. 2).

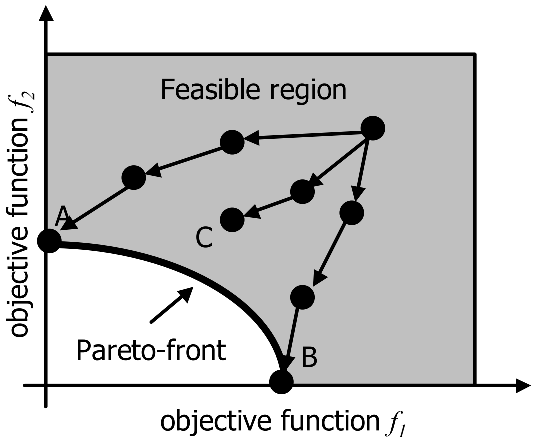

Figure 2. Weighted-sum method applied to a MOP having a concave Pareto-front. *Any combination of weights a_1 and a_2 would results in the extreme optimum A or B. A gradient-based method may be stacked at a local optimum C due to complexity of the objective function distributions.*

Evolutionary Algorithms[6] (EAs) are design optimization algorithms based on the *Theory of Evolution* proposed by Charles Darwin, where a biological population evolves over generations to adapt to an environment by selection, recombination and mutation. EAs are particularly suited for MOPs because they can uniformly sample various Pareto-optimal solutions in one optimization without converting a MOP into a single objective problem by maintaining a population of design candidates and using a fitness assignment method based on the Pareto-optimality concept[6]. In addition, EAs have other advantages such as robustness, efficiency, as well as suitability for parallel computing. Due to these advantages, EAs are enjoying popularity in multidisciplinary design optimizations[1,3,4,and 7].

EAs, however, do not have any explicit mechanism to handle design constraints. Traditional approach for handling design constraints of a single-objective design optimization problem is the penalty function method[6] where fitness of a design candidate is determined based on a scale function *F*, which is weighted sum of the objective function value $f_1$and the amount of design constraint violations $g_n \ (1 \le n \le n_{\max})$

$$F(\vec{x}) = f_1(\vec{x}) + \sum_{n=1}^{n_{\max}} b_n \cdot \max(g_n(\vec{x}),0) \tag{2}$$

where b_n is negative for maximization problems and positive for minimization problems.

However, this method requires a careful tuning of the penalty function coefficients to obtain a global optimum. For example, if the penalty function coefficients are too small, the optimized design would not satisfy the constraints. On the other hand, if the penalty function coefficients are too large, the optimized design would not have satisfactory objective function value. Balance between the constraints is also important. If the coefficient of some penalty functions is too small, these constraints would not be satisfied. In addition, the penalty function method is not intended to deal with multiobjective design optimization problems. Application of this method to a multiobjective optimization problem also give rise to another problem - how to combine multiple constraints with multiple objectives.

Deb proposed an attracting approach[8] for constraint-handling which bases on the non-dominance concept where feasible designs dominate infeasible designs. This approach does not need tuning of the penalty function coefficients as long as the number of constraint is one. In this sense, this approach is very useful for EA-based design optimizations. However, this approach still requires careful tuning of the weight coefficients of the constraints when multiple constraints are considered. Coello[9] and Coello and Mezura[10] also proposed non-dominance-based constraint-handling techniques, which does not use any coefficient to be tuned even if multiple constraints are considered. However, these techniques may not be very efficient when the degrees of violation of constraints are significantly different because these techniques do not always consider balance between constraint violations of infeasible designs.

The objective of the present study is to propose a new efficient and robust constraint-handling method for multiobjective and multi-constraint design optimization problems. The proposed method defines fitness of a design candidate by applying the Pareto-optimality concept to constraints of the design where rank of an infeasible solution is defined by Pareto-ranking among entire population. As a result, the proposed method does not need tuning of any coefficients and is efficient and robust even when degrees of constraint violations are significantly different. First, the optimal design of a welded beam and a multidisciplinary conceptual design optimization of a two-stage-to-orbit space plane are demonstrated to compare the proposed method with the traditional penalty function approaches. Then, a high-fidelity aerodynamic design optimization of an axial compressor blade involving constraints on thickness distribution is demonstrated by using the proposed approach.

II. The Proposed Constraint-Handling Method

In the proposed constraint-handling method, the Pareto-optimality concept, which is usually applied to the objective function space for EA-based design optimizations, is applied to the constraint function space. Fitness of a design candidate is determined by its rank among entire population, which is determined according to the following non-dominance concept:

Definition 1: A solution *i* is said to constrained-dominate a solution *j*, if any of the following conditions is true:
Solutions *i* and *j* satisfy all constraints and solution *i* dominates solution *j* in objective function space.
Solution *i* satisfies all constraints and solution *j* does not.
Solutions *i* and *j* do not satisfy any of the constraints, but solution *i* dominates solution *j* in constraint space.

where dominance in objective function space is defined as **Definition 2** while dominance in constraint space is defined as **Definition 3**:

Definition 2: A solution *i* is said to dominate a solution *j* in objective function space, if both of the following conditions are true:
Solutions *i* is no worse than solution *j* in all objectives, *i.e.,*

$$\forall f_m(\vec{x}_i) \le f_m(\vec{x}_j) \tag{3}$$

Solution *i* is strictly better than solution *j* in at least one objective, *i.e.,*

$$\exists f_m(\vec{x}_i) < f_m(\vec{x}_j) \tag{4}$$

Definition 3: A solution *i* is said to dominate a solution *j* in constraint space, if both of the following conditions are true:
Solutions *i* is no worse than solution *j* in all constraints, *i.e.*,

$$\forall G_n(\vec{x}_i) \le G_n(\vec{x}_j) \tag{5}$$

Solution *i* is strictly better than solution *j* in at least one constraint, *i.e.*,

$$\exists G_n(\vec{x}_i) < G_n(\vec{x}_j) \tag{6}$$

where

$$G_n(\vec{x}) = \max(0, g_n(\vec{x})) \tag{7}$$

The advantage of the proposed method is that it does not need any coefficient to be tuned. In addition, efficiency of the evolutionary algorithm is not affected by difference in the degree of violation of each constraint. The proposed algorithm is also robust by maintaining diversity in the population while no feasible design is found in the initial phase of the optimization.

The proposed constraint-handling technique can be used with any kind of evolutionary algorithm. The present EA uses the floating-point representation[11] to represent design parameters of design candidates where an individual is characterized by a vector of real numbers. Random parental selection and the best-*N* selection[12] where the best *N* individuals are selected for the next generation among *N* parents and *N* children based on Pareto-optimality defined in Definition 1. The blended crossover[13] is used for reproduction. Since the strong elitism is used, high mutation rate of 0.2 is applied and a random disturbance is added to the parameter in the amount up to ±20% of the design space. The initial population is generated randomly over the entire design space.

III. Optimal Design of a Welded Beam

In this chapter, the present EA coupled with the proposed constraint-handling technique is compared with the same EA coupled with the penalty function approach by deb[8], the approach by Coello[9], or, a penalty function method by demonstrating optimal design of a welded beam[14]. The present penalty function method to be compared with the proposed constraint-handling method is the dynamic penalty method proposed by Joines and Houck[15]. In the dynamic penalty method, fitness of each solution is determined by the following function;

$$F(\vec{x}) = f_1(\vec{x}) + (C \cdot t)^{\alpha} \cdot \left(\sum_{n=1}^{n_{\max}} G_n^{\beta}(\vec{x}) \right) \tag{8}$$

where t is generation and C, α and β are constants defined by the user ($C = 0.5$, $\alpha = 2$ and $\beta = 2$ were used) . This dynamic function approach is considered to be efficient in the sense that number of coefficients to be tuned is small as well as the penalty function coefficient changes through out generations to increase the penalty as the optimization progresses.

A. Formulation of the Design Optimization Problem

Structure of the welded beam is shown in Fig. 3. The welded beam consists of a beam and a weld required to secure the beam to the member. The objective of the design is to find a feasible set of dimensions *h, l, t*, and *b* to carry a certain load (*P*) and still have a

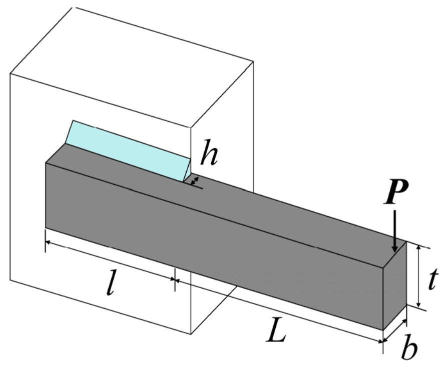

Figure 3. The welded beam structure.

minimum total fabricating cost. Detail of the problem is described in Ref. 14. The maximum bending stress and the maximum shear stress of the present design problem are smaller than those of the original one to give severer constraints to compare the constraint-handling techniques.

B. Result

Population size and number of generations are set to 100 and 200, respectively. Fifty trials starting from different initial populations are demonstrated to statistically compare the constraint-handling methods. Since severe constraints are imposed on the present optimization problems, the evolutionary algorithm sometimes failed to find feasible designs. Table 1 shows the number of trials in which feasible designs are found and the average cost of the optimized designs. It is remarkable that the present constraint-handling technique found feasible designs 48 times among 50 trials. The average cost of the designs optimized by the EA coupled with the proposed method is also smaller than the EA coupled with the other function methods.

Table 1 Result of the welded beam design optimization

	Number of trials in which feasible solutions are found	Average cost
Proposed method	48	5.60
Method by Coello	31	5.75
Method by Deb	38	5.63
Penalty method	42	5.68

IV. Multidisciplinary Conceptual Design Optimization of a Single-Stage-To-Orbit Spaceplane

In this section, multidisciplinary conceptual design optimization of a two-stage-to-orbit (TSTO) spaceplane is demonstrated to ensure feasibility of the present approach to multidisciplinary design optimization problems. The TSTO spaceplane considered here consists of a booster with air-breathing engines and an orbiter with rocket engines. The orbiter is separated from the booster at a certain altitude and reaches the low earth orbit (LEO) to release the payload.

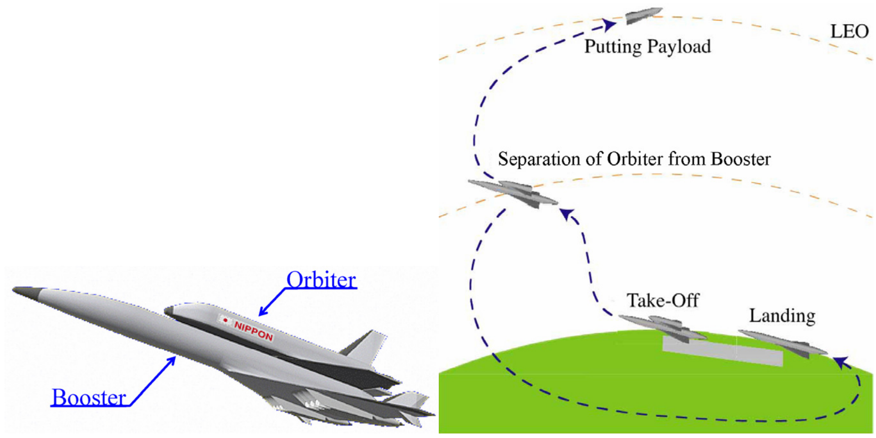

Figure 4. The TSTO Spaceplane and its mission.

A. Formulation of the Design Optimization Problem

The present TSTO mission is to put a payload of 10t into the equatorial orbit at the altitude of 400km. For simplicity, the take-off and landing sites are assumed to be on the equator. The engine of the Booster is assumed to be the air-turbo-ramjet engine with expander cycle[16] (ATREX), which is under development in Japan. The objective is to minimize gross take-off weight of the spaceplane. The separation time is constrained to be smaller than 550 seconds. The maximum thrust of the booster is also constrained to be smaller than 2.5 (MN). The gross take-off weight, separation time and maximum thrust of the booster are iteratively computed from the propulsion, aerodynamics, trajectory and structure modules[17,18]. Here, propulsion, trajectory and airframe configuration parameters (total ten) are considered as design variables.

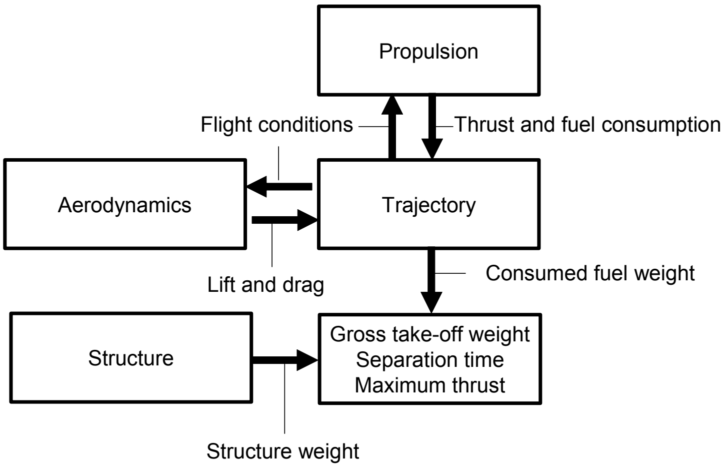

Figure 5. The TSTO simulation system.

B. Result

Population size and number of generations are set to fifty. One hundred trials with different initial populations are run for each constraint-handling technique. Table 2 presents number of trials in which feasible designs are found, the average weight of the optimized designs and the standard deviation. The penalty method and dominance-based approach by Deb failed to find feasible designs. The reason is probably that both methods adopt linear-sum of the amount of constraint violation of different order of magnitude. The present method found feasible designs every trial while the method by Coello failed once. In addition, the average weight of the optimized designs and standard deviation of the present method are smaller than those of the method by Coello.

Table 2. Result of the TSTO design optimization

	Number of trials in which feasible solutions are found	Average weight, Mton	Standard deviation, ton
Proposed method	100	0.37119	1578.7
Method by Coello	99	0.37129	1623.9
Method by Deb	No feasible design is found		
Penalty method	No feasible design is found		

V. High-Fidelity Aerodynamic Design Optimization of an Axial Compressor Blade

A. Formulation of the Design Optimization Problem

The optimization problem considered here is to seek a redesign of NASA rotor67[19], which is a low-aspect-ratio transonic axial-flow fan rotor and is the first-stage rotor of a two-stage fan. The fan was designed and tested to help provide the technology to develop efficient, lightweight engines for short-haul aircraft in 1970s. The rotor 67 was designed by using a streamline-analysis computational procedure, which provides an axisymmetric, compressible-flow solution to the continuity, energy, and radial equilibrium equations.

The rotor design pressure ratio is 1.63 at a mass flow of 33.25 kg/sec. The design rotational speed is 16043 rpm, which yields a tip speed of 429 m/sec and an inlet tip relative Mach number of 1.38. The rotor has 22 blades and aspect ratio of 1.56 (based on average span/root axial chord). The rotor solidity varies from 3.11 at the hub to 1.29 at the tip. The inlet and exit hub/tip radius ratios are 0.375 and 0.478, respectively. Reynolds number is 1.797M based on the blade axial chord at the hub.

The objective of the aerodynamic rotor shape design optimization problem is to minimize the flow loss manifested via entropy generation. Here, mass-averaged entropy production from inlet to exit at the design point of rotor67 is considered as the objective function to be minimized. Because an optimized rotor design should meet the required mass flow rate and pressure ratio, they are maintained by specifying constraints on them:

$$\left|\frac{massflowrate_{design} - massflowrate_{rotor67}}{massflowrate_{rotor67}}\right| \leq 0.005 \quad (9)$$

$$\left|\frac{pressureratio_{design} - pressureratio_{rotor67}}{pressureratio_{rotor67}}\right| \leq 0.01 \quad (10)$$

In addition, thickness of the optimized design is constrained to be equal to or larger than that of the rotor 67:

$$\sum \max(0, thickness_{rotor67} - thickness_{design}) \leq 0 \quad (11)$$

where thicknesses of the designs and rotor 67 are measured at 10%, 20%, …, 90% chord positions on 57 blade profiles from root to tip.

B. Approach

1. Blade Shape Parameterization

Here a rotor blade shape is represented by four blade profiles, respectively at 0%, 31%, 62%, and 100% spanwise stations (all spanwise locations discussed here are measured from the hub), the spanwise twist angle distribution, and the stacking line. Each of these sectional profiles can be uniquely defined by using a mean camber line and a thickness distribution. Here, they are parameterized by the third-order B-Spline curves and positions of control points of the B-Spline curves are considered as the design parameters. As illustrated in Fig. 6, five control points are used for the mean camber line. For the thickness distribution, two control points are added at the leading edge and the trailing edge so that these points represent leading edge and trailing edge radii, respectively. Chordwise locations of the control points at leading edge and trailing edge are frozen to zero and one, respectively. The thickness control points at the leading and trailing edges are defined so that the leading and trailing radii of the designs are identical to those of the rotor 67. These profiles are linearly interpolated from hub to tip.

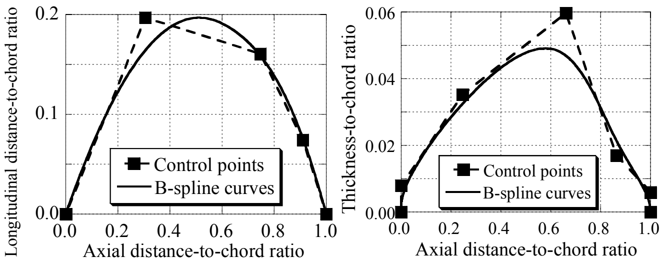

Figure 6. B-Spline curves for mean camber line and thickness distribution.

Stagger angles are defined at 0%, 33%, 67%, and 100% spanwise stations and linearly interpolated. Spanwise chord length distribution remains identical to that of the rotor 67. Final Blade shape is defined by stacking the blade profiles around the center of gravity of each profile. Here, streamwise and circumferential the stacking lines are defined by B-Spline curves as shown in the Fig. 7, respectively. As a result, each blade shape is represented with 49 design parameters.

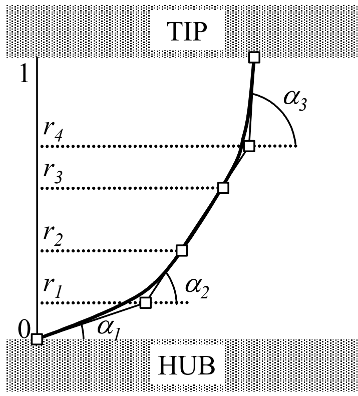

Figure 7. Stacking line definition.

2. Three-Dimensional Navier-Stokes Solver

The three-dimensional Navier-Stokes (N-S) code used in the present research is TRAF3D[20,21]. Capability of the present code has been validated by comparing the computed results to some experiments such as the Goldman annular vane with and without end wall contouring, the low speed Langston linear cascade[20] as well as the NASA rotor67[21].

TRAF3D solves the three-dimensional full Reynolds-averaged N-S equations. It uses a central-differencing scheme including artificial dissipation terms introduced by Jameson, Schmidt, and Turkel[22] to maintain stability and to prevent oscillations near shocks or stagnation points. In order to minimize the amount of artificial diffusion inside the shear layer, the eigenvalues scaling of Martinelli[23] and Swanson and Turkel[24] are incorporated. The two-layer eddy-viscosity model of Baldwin and Lomax is adopted for the turbulence closure. The system of the differential equations is advanced in time using an explicit four-stage Runge-Kutta scheme. In order to accelerate convergence of calculations, local time-stepping, implicit residual smoothing[25], and the Full Approximation Storage multigrid technique[26] are adopted.

At the subsonic axial inlet, the flow angles, total pressure and total enthalpy are specified according to the theory of characteristics while the outgoing Riemann invariant is taken from the interior. At the subsonic axial outlet, the average value of the static pressure at the hub is prescribed and the density and components of velocity are extrapolated together with the circumferential distribution of pressure. The radial equilibrium equation is used to determine the spanwise distribution of the static pressure. On sidewalls, the momentum equation, the no-slip condition, and the temperature condition are used to compute pressure and density. For the calculations presented in this paper, all the walls have been assumed to be adiabatic. The periodicity from blade passage to blade passage is imposed by setting periodic phantom cell values. At the wake, where the grid is not periodic, the phantom cells overlap the real ones. Linear interpolations are then used to compute the value of the dependent variables in phantom cell.

The three-dimensional grids are obtained by stacking two-dimensional grids generated on the blade-to-blade surface. These two-dimensional grids are of C-type and are elliptically generated, with controlled grid spacing and orientation at the wall. The problem of grid skewness due to high stagger or large camber is addressed by allowing the grid to be non-periodic on the wake[27]. By adding lines near the wall, viscous grids are obtained from the inviscid grids. The wall normal spacing scaled with the axial chord is 10^{-4}. In the spanwise direction a standard H-type structure has been adopted. Near the hub and tip walls geometric stretching is used for a specified number of grid points, after which the spanwise spacing remains constant. The number of the grid points is 201 chordwise x 53 tangential x 57 spanwise. Among the 201 chordwise grid points, 149 grid points are distributed along the blade shape. The computational grid for the NASA rotor 67 is shown in Fig. 8.

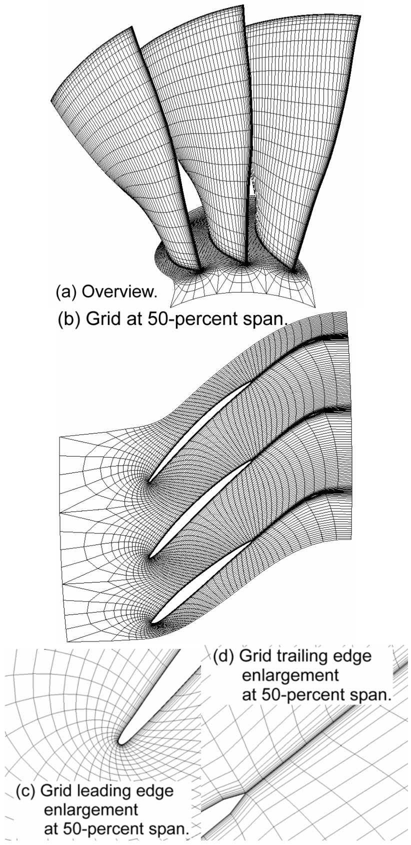

Figure 8. Computational grid over NASA rotor67. Every other line is

In the present study, all computations are performed on the NEC SX-6 machine consisting of 128 vector processing elements (PEs) located at JAXA Institute of Space and Astronautics Science in Japan. Aerodynamic evaluations of design candidates at each generation is parallelized using the simple master-slave concept; the grid generations and the flow calculations associated to the design candidates of a generation are distributed into 32 PEs of the NEC SX-6 machine.

C. Result

Population size and number of generations are set to sixty-four and fifty, respectively. Figure 9 presents optimization history in terms of the objective function (entropy production) compared with the NASA rotor 67 and optimization history by Deb's approach where constraint violation *CV* is defined as

$$CV = 2 \cdot CV_{massflowrate} + CV_{pressureratio} \tag{12}$$

The optimized designs obtained after the eighth generation satisfied all the constraints. The final design has smaller entropy production than the NASA rotor 67 while the optimized design by Deb's approach does not. Further optimization may result in a better design.

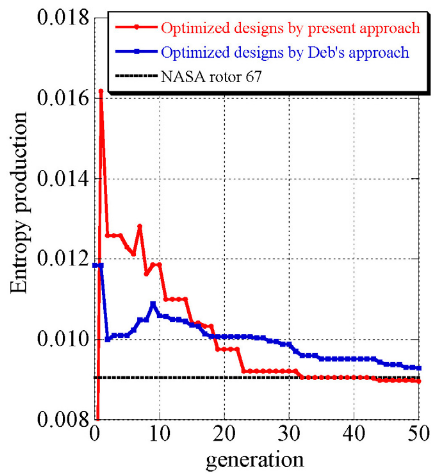

Figure 9. Optimization histories.

Figures 10 and 11 compare spanwise leading-edge sweep and lean distributions of the optimized design and the NASA rotor 67. The optimized design has larger backward sweep than the NASA rotor 67 to reduce entropy production due to shock wave. The optimized design also has larger lean toward pressure side hear hub.

Figure 12 compares stagger angle distributions. Although the distributions are qualitatively almost identical, the optimized design has larger stagger angle. The blade profiles of the optimized design and rotor67 are shown in Fig. 13.

Spanwise entropy distributions of the optimized design and the NASA rotor 67 are compared in Fig. 14. The figure shows that the entropy production is reduced mainly between 60% to 90% span while it is increased near the tip.

Figures 15 and 16 compare blade profiles and surface static pressure distributions at 67%, and 90% spanwise stations, respectively. These figures indicate that the optimized design has thicker thickness distribution than the NASA rotor 67 to satisfy the strict constraint on the thickness distribution. While thicker profile generally increases entropy production due to shock wave, the optimized design avoided significant increase in entropy production by increasing axial sweep.

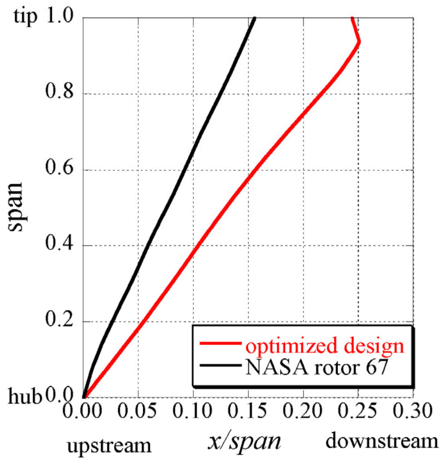

Figure 10. Axial sweep distributions.

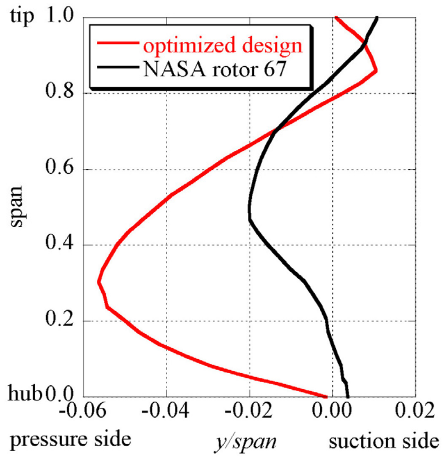

Figure 11. Circumferential lean distributions.

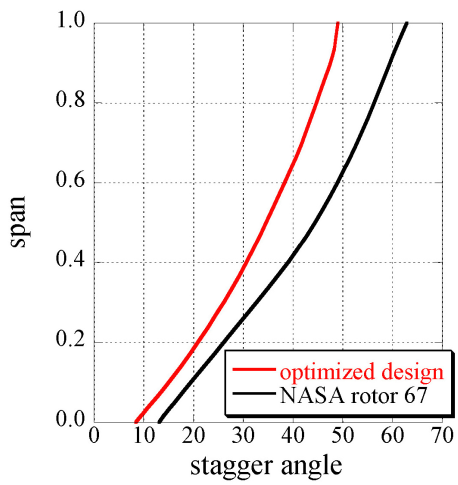

Figure 12. Stagger angle distributions.

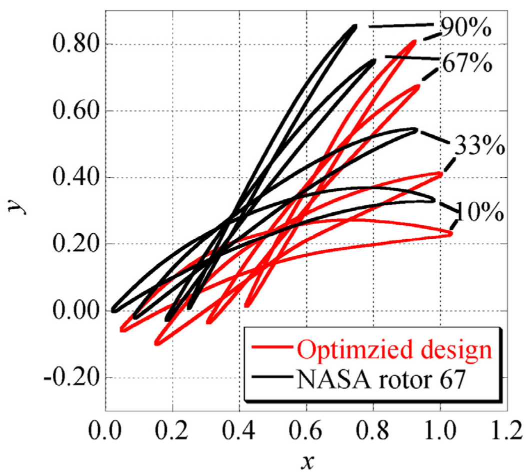

Figure 13. Blade profiles of the optimized design and the rotor 67.

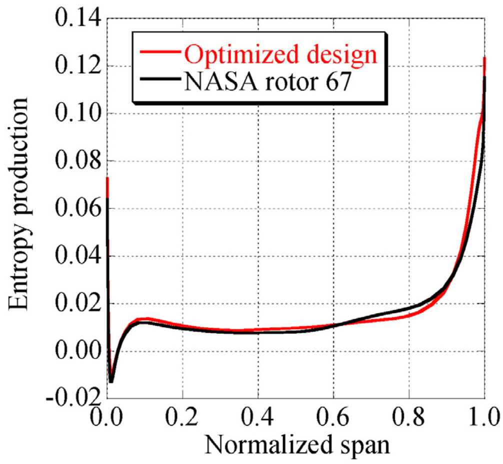

Figure 14. Comparison of the spanwise entropy distributions.

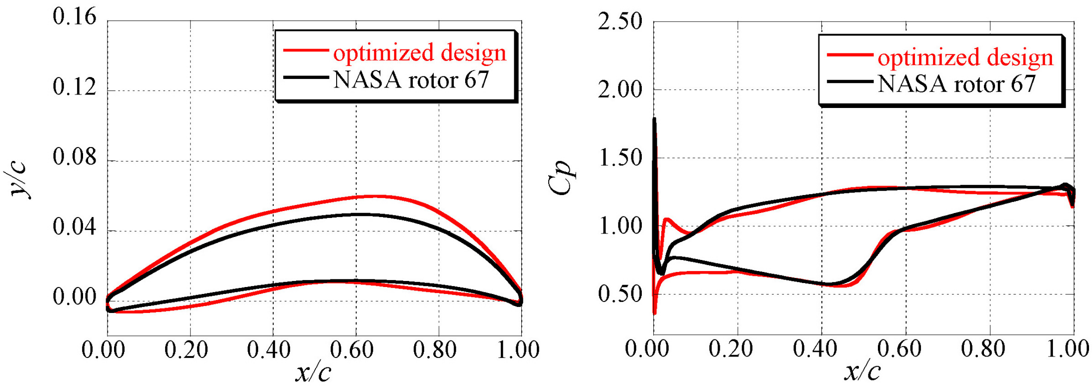

Figure 15. Comparison between the optimized design and the rotor 67 at 67% span.

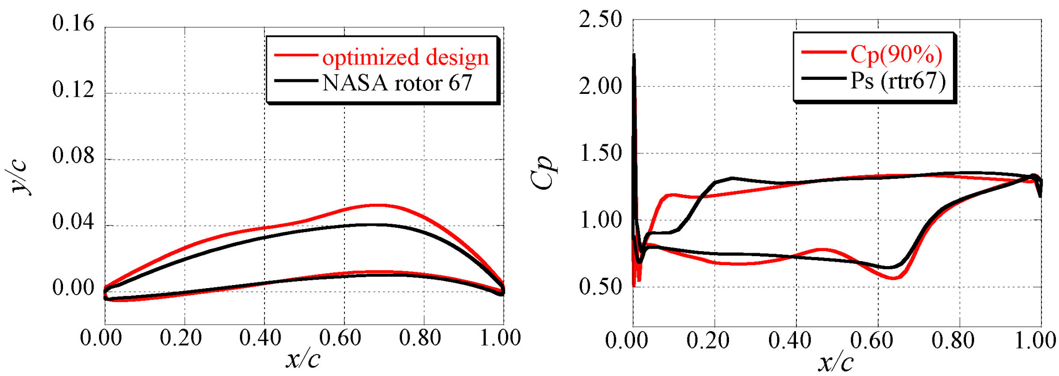

Figure 16. Comparison between the optimized design and the rotor 67 at 90% span.

VI. Conclusion

A new constraint-handling technique based on the Pareto-optimality concept has been proposed for evolutionary algorithms to efficiently deal with multiobjective multi-constraint design optimization problems. The essence of the proposed method is to apply non-dominance concept based on constraint function values to infeasible designs and to apply non-dominance concept based on objective function values to feasible designs. Unlike traditional penalty function methods, the proposed technique does not need any constants to be tuned as the proposed technique does not use weighted-sum of constraints.

The proposed approach was demonstrated to be remarkably more robust than a traditional penalty function method through the optimal design of a welded beam and conceptual design optimization of a two-stage-to-orbit spaceplane. Although these problems are single-objective design optimizations, application of the present method to multiobjective multi-constraint design optimization problem is straightforward. In addition, implementation of the proposed approach to a multiobjective evolutionary algorithm is very easy because the Pareto-based ranking is already implemented in most of multiobjective evolutionary algorithm codes.

Next, high-fidelity aerodynamic design optimization of an axial compressor design optimization was also demonstrated. The present EA coupled with the proposed approach successfully found a design that has smaller entropy production than the NASA rotor 67 and satisfies constraints on mass flow rate, pressure ratio, and thickness distribution. Due to the strict constraints on thickness distribution, the optimized design did not get significant reduction in entropy production. Multiobjective and multidisciplinary (aerodynamics and structural dynamics) design optimization may be necessary to design an innovative blade.

References

[1] Sasaki, D., Obayashi, S. and Nakahashi, K. "Navier-Stokes Optimization of Supersonic Wings with Four Objectives Using Evolutionary Algorithm," *Journal of Aircraft*, Vol. 39, No. 4, 2002, pp. 621-629.

[2] Choi, S., Alonso, J. J., Kroo, I. M., and Wintzer, M., "Multi-Fidelity Design Optimization of Low-Boom Supersonic Business Jets," CD-ROM proceedings of 10th AIAA/ISSMO Multidisciplinary Analysis and Optimization Conference, AIAA paper 2004-4371, 2004.

[3] Duranté, N., Dufor, A., Pain, V., Baudrillard, G. and Schoenauer, M., "Multidisciplinary Analysis and Optimization Approach for the Design of Expendable Launchers," CD-ROM proceedings of 10th AIAA/ISSMO Multidisciplinary Analysis and Optimization Conference, AIAA paper 2004-4441, 2004.

[4] Oyama, A., and Liou, M.-S., "Multiobjective Optimization of a Multi-Stage Compressor Using Evolutionary Algorithm," Proceedings of AIAA/ASME/SAE/ASEE Joint Propulsion Conference & Exhibit, AIAA paper 2002-3535, 2002.

[5] Vanderplaats, G. N., *Numerical Optimization Techniques for Engineering Design*, McGraw-Hill Book Company, New York, NY, 1984.

[6] Deb, K., *Multi-Objective Optimization Using Evolutionary Algorithms*, John Wiley & Sons, Chickester, England, 2001.

[7] Shimoyama, K., Fujii, K., and Kobayashi, H., "Development of Realistic Optimization Method of TSTO Spaceplane – Multi-Objective and Robust Optimization," CD-ROM proceedings of 10th AIAA/ISSMO Multidisciplinary Analysis and Optimization Conference, AIAA paper 2004-4475, 2004.

[8] Deb, K., "An Efficient Constraint-handling Method for Genetic Algorithms," *Computer Methods in Applied Mechanics and Engineering*, Vol. 186, No.2-4, 2000, pp.311-338.

[9] Coello, C. A. C., "Constraint-Handling Using an Evolutionary Multiobjective Optimization Technique," *Civil Engineering and Environmental Systems*, Vol. 17, 2000, pp.319-346.

[10] Coello, C. A. C. and Mezura-Montes, E., "Constraint-Handling in Genetic Algorithms Through the Use of Dominance-Based Tournament Selection," *Advanced Engineering Informatics*, Vol. 16, 2002, pp.193-203.

[11] Michalewicz, Z., *Genetic Algorithms + Data Structures = Evolution Programs, Third, Revised and Extended Edition,* Sprinter-Verlag, Berlin Heidelberg New York, 1996.

[12] Tsutsui, S., and Fujimoto Y., "Forking Genetic Algorithms with Blocking and Shrinking Modes (fGA)," *Proceedings of the Fifth International Conference on Genetic Algorithms*, Morgan Kaufmann Publishers, Inc., San Mateo, CA, pp.1993, pp.206-213.

[13] Eshelman, L. J., and Schaffer, J. D., "Real-Coded Genetic Algorithms and Interval Schemata," *Foundations of Genetic Algorithms.2,* Morgan Kaufmann Publishers, Inc., San Mateo, CA, 1993, pp.187-202.

[14] Deb, K, "Optimal Design of a Welded Beam via Genetic Algorithms," *American Institute of Aeronautics and Astronautics Journal,* Vol. 29, No. 11, 1991, pp.2013-2015.

[15] Joines, J., and Houck, C., "On the Use of Non-Stationary Penalty Functions to Solve Nonlinear Constrained Optimization Problems with Gas," *Proceedings of the First IEEE Conference on Evolutionary Computation,* IEEE Press, Orlando, FL, 1994, pp. 579-584.

[16] Tanatsugu, N., and Carrick, P., "Earth-to-Orbit Combined Rocket/Airbreathing Propulsion," AIAA Paper 2003-2586, 2003.

[17] Kobayashi, H, and Tanatsugu, N., "Optimization Method on TSTO Spaceplane System Powered by Airbreather," AIAA Paper 2001-3965, 2001.

[18] Shimoyama, K., Fujii, K., and Kobayashi, H., "Improvement of the Optimization Method of the TSTO Configuration – Application of Accurate Aerodynamics," Proceedings of Third International Conference on Computational Fluid Dynamics, 2004.
[19] Walter, S. C., William, S., and Donald, C. U., "Design and Performance of a 427-Meter-Per-Second-Tip-Speed Two-Stage Fan Having a 2.40 Pressure Ratio," NASA TP-1314, October 1978.
[20] Arnone, A., Liou, M.-S., and Povinelli, L. A., "Multigrid Calculation of Three-Dimensional Viscous Cascade Flows," NASA TM-105257, ICOMP-91-18, 1991.
[21] Arnone, A., "Viscous Analysis of Three-Dimensional Rotor Flow Using a Multigrid Method," *ASME Journal of Turbomachinery*, Vol. 116, July 1994, pp. 435-445.
[22] Jameson, A., Schmidt, W., and Turkel, E., "Numerical Solutions of the Euler Equations by Finite Volume Methods Using Runge-Kutta Time-Stepping Schemes," AIAA Paper 1981-1259, 1981.
[23] Martinelli, L. and Jameson, A., "Validation of a Multigrid Method for the Reynolds Averaged Equations," AIAA Paper 1988-0414, 1988.
[24] Swanson, R. C., and Turkel, E., "Artificial Dissipation and Central Difference Schemes for the Euler and Navier-Stokes Equations," AIAA Paper 1987-1107, 1987.
[25] Jameson, A., "The Evolution of Computational Methods in Aerodynamics," *Journal of Applied Mech*anics, Vol. 50, 1983, pp. 1052-1069.
[26] Jameson, A., "Transonic Flow Calculations," MAE Report 1651, MAE Department, Princeton University, July 1983.
[27] Arnone, A., Liou, M.-S., and Povinelli, L. A., "Transonic Cascade Flow Calculations Using Non-Periodic C-Type Grids," Computational Fluid Dynamics Symposium on Aeropropulsion, NASA Lewis Research Center, Cleveland, April, 1990.